A Robust and Accurate Detection of Pupil Images

Lin Lin Lin Pan LiFang Wei Lun Yu
College of Physics & Information Engineering
Fuzhou University
Fuzhou, China

***Abstract*—Precise pupil features detection is an important factor for screening diabetic retinopathy. Some interferences caused by reflections, eyelashes and eyelids in pupil extraction need to be solved. This paper presents an algorithm to precisely estimate pupil features: pupil center and pupil radius. The system's hardware component allows for high frame rate image acquisition under infrared lighting conditions. We use several real time image processing techniques to estimate the pupil size under the influence of corneal reflection and eyelid occlusion conditions. The experimental results show a good robustness and accuracy.**

Keywords-diabetic retinopathy; image processing; ROI; pupil extraction；pupil center

I. INTRODUCTION

Diabetic Retinopathy (DR) is one of the potential chronic complications of diabetes that may cause blindness. The blindness rate caused by DR is 25 times that of the non-diabetic patients. And DR is becoming the major blinding eye diseases for 20s-70s [1]. With the increasing age, the risk of blinding eye disease becomes greater. Since early detection and early treatment can slow down even prevent the blindness, experts suggest that it's better to screen for eye disease for the high-risk groups with family history of diabetes every year.

The method of using pupil response to screen DR was initially proposed by Gorin in 2006 [2]. Compared to existing methods including examination by the ophthalmologist using ophthalmoscope or slit-lamp pre-focusing mirror directly, a digital image obtained through the fundus photography for retinopathy evaluating could be an ideal examine method. The former two screening methods are subjective and can not be recorded for it is observed by the ophthalmologist directly, whereas fundus camera of special optical design is able to capture clear images with digital interface, making it an effective tool for screening [3]. Image captured by fundus camera has the advantages that it provides an objective test result, is fast, non-invasive, easy to use.

With mydriatic fundus imaging one can get a large field of view, which makes it better for fluorescence angiography for accurate diagnosis. But it needs time and may bring complications at the same time, and some patients who have glaucoma can not be dilated. On the other hand, nonmydriatic fundus imaging provides convenience to patients as it does not need to dilate, but the field of view is so small, about 20-45 degrees, that it affects the accuracy of the screening. As a result, we need to take the multi-angle shooting into account. However, most exiting eye tracking systems focus on the improvement of accurate measurement of pupil center, and measurement of pupil center in a wide angle and of the pupil diameter were not considered sufficiently.

We observed that droopy eye lids partially covering the pupil is a quite common phenomenon. But most existing pupil size estimation systems either assume the artifacts, including cornea reflex and eye lid occlusion, are negligible, or are not designed to detect the pupil change in real time [4]. This paper presents an accurate pupil center and pupil size detecting algorithm in a multi-angle shooting which ensure both real time performance and robustness. The algorithm assumes that the pupil appears as a circle at the central position and looks elliptical when at eccentric positions.

II. SYSTEM OVERVIEW

Our aim is to generating multi-angle shooting images for processing, so both the accurate pupil positioning and the accurate pupil diameter measurement is important. The pupil positioning corresponds to the location of the incident light. If the pupil does not have the right position, the light beam will not shine eyes, resulting in vague retinal imaging. And the effective pupil diameter measurement corresponds to the luminous flux of incident light. The luminous flux into the eyes can be controlled by the size of the pupil. Thus we can take the effective pupil diameter measurement as a criterion for determining whether the image captured is fit for processing or not.

Infrared light-emitting diodes are used in our system, whose infrared light reflects from the pupil to the CCD video camera for imaging. There are two types of imaging processes, visible and infrared spectrum imaging [5]. The best feature to track in visible spectrum images captured by the cameras is the contour between the iris and the sclera. In this case, ambient light may reflect from the eye and uncontrolled specular diffuse may occur at the same time. Infrared spectrum imaging eliminates uncontrolled specular reflection by actively illuminating the pupil with a uniform, and the pupil, rather than the iris, is the strongest feature contour in the image. The reason is that both the sclera and the iris strongly reflect infrared light while only the sclera strongly reflects visible light.

We use dark-pupil techniques in our system. It illuminates the eye with an off-axis source such that the pupil is the darkest region in the image, while the sclera, iris and eye lids all reflect

978-1-4244-6498-2/10/$26.00 ©2010 IEEE

relatively more illumination. We use infrared off-axis lighting for image acquisition to produce a black pupil effect so that the pupil area is easy to extract.

It is necessary to detect an ellipse rather than a circle for tracking the pupil due to the position of the camera. When looking in the direction of the camera, the pupil appears as a circle. However, when looking in another direction, the pupil looks like ellipse. The software block diagram is shown in Fig. 1, according which we locate the pupil center and calculate the pupil diameter.

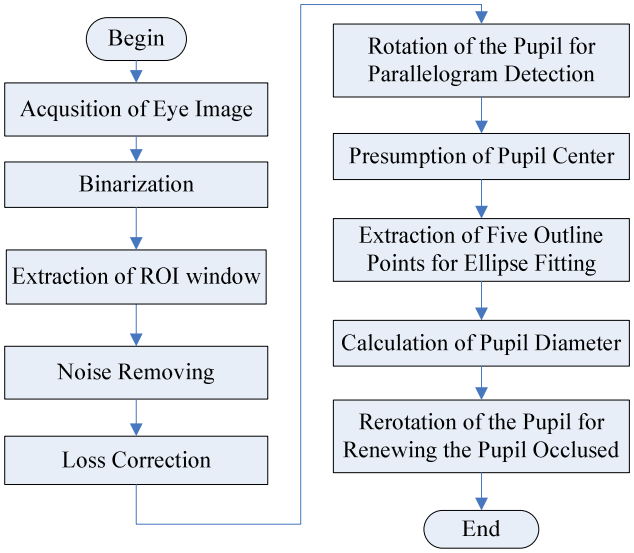

Figure 1. The software block diagram

III. IMAGE PROCESSING FOR PUPIL DIAMETER MEASUREMENT

A. *Pupil Segmentation*

Images are captured first at full size and full resolution (320×240), and then transformed into binary images at a user-set threshold. The images are divided into two parts. One is the background, whose gray-level is under the threshold and labeled as "one". The other is the object pixels, whose gray-level is up the threshold and labeled as "zero".

After the binary procedure, the approximate pupil center is located by the center of mass algorithm, and then a tiny image window is specified slightly larger than the detected pupil area for further processing so that we do not lose any pixels. A 120 × 90 pixel Region of Interest (ROI) window downsampled at 1/4 1/4 rate of the original resolution is enough for capturing the whole pupil. We process the tiny image at full pixel density resolution using the algorithm described below to locate the accurate position of the pupil center, shown in Fig. 2. By selecting the ROI window, we can reach an even higher speed. In addition to the processing time, computation cost of capturing the image and image displaying also slow down the overall frame rate.

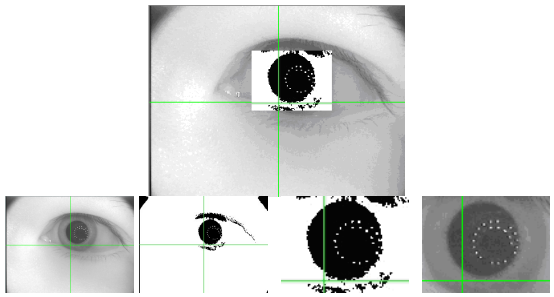

Figure 2. The upper row shows a full pixel density resolution grey level image (the partial image defined by the ROI window), with the small threshold image inlayed on the right location. The lower row shows, from left to right, the down sampled grey level image, the threshold image of the downsampled image, the small threshold image in the tiny trace window, and the grey level image of full pixel density resolution in the tiny trace window.

B. *Corneal Reflection and Noise Removal*

Because of the spots causing by the corneal reflex, there exists some missing areas, indicated by white pixels. The X-axis coordinate that changes from white to black in the direction of X-coordinate in each Y-coordinate is to be detected beforehand and is considered as a candidate for the boundary at the left of the pupil. On the contrary, the farthest X-coordinate that changed from white to black in the opposite direction of X-coordinate is considered to be a candidate for the boundary at the right of the pupil. Then it can be filled in with black pixels from the left boundary to the right boundary, as shown in Fig.

Figure 3. The loss area is removed in the X and Y direction.

3.

Similarly, the missing areas of the pupil can be further reduced by performing this procedure in the Y direction, as shown in Fig. 3. This raises the accuracy.

We note that it is best to remove the grain noise before adopting this method, or we will find the wrong dots as the boundary and appears to expand the pupil area because of

Figure 4. At left is the binary pupil with noise. At right is the result of loss correction without noise removing.

individual particles, as shown below.

The problem is that it will cause a lot of limbic protrusions when most spots concentrated in the edge of the pupil, thus results in a bad treatment effect, as shown below.

Figure 5. At left is the binary pupil with the spots concentrated in the edge of the pupil. At right is the result of loss correction using the principle.

C. *Presumption of Pupil Center*

According to the geometric nature, we know that the center of the parallelogram inscribed in the same ellipse corresponds to the center of another inscribed parallelogram [6]. Therefore, the center of the parallelogram inscribed in the ellipse can be taken as the center of the ellipse.

Regarding the pupil edge detection error, the center may not always coincide in one point. Therefore, it needs to repeat the construction of the entire inscribed parallelogram, and take the point which coincidence the most times as the center. Since it needs to calculate the mid-point time after time and do the comparing, this increases the computation and is time-consuming.

As shown in the left-hand side of Fig. 6, we can find that the centers of the parallelogram inscribed in the ellipse are the same which can serve as the center of the ellipse, but for the ellipse which has some missing areas because of corneal reflex, as shown in the right-hand side of Fig. 6. When the missing corner makes part of the vertices of a parallelogram, the center of the parallelogram has discrepancies with others, which can be removed. Thus, this method can effectively solve the problem of missing area caused by the corner spot reflection, and has a high stability.

Figure 6. At left, the centers of the correct parallelograms that are inscribed on the elllilpse are gathered in one place, which can be taken as the center of the ellipse. At right, the center of the incorrect parallelogram (blue parallelogram) is located in far from the others.

Fig. 7 shows the experimental results, we can see that, when the pupil is occluded, the midpoint obtained by the center of gravity method is not accurate, while using the inscribed parallelogram method the midpoint obtained is more accurate without the impact of blocked, and has a higher accuracy and stability.

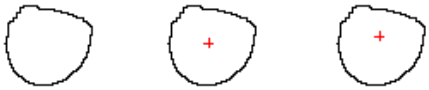

Figure 7. From left to right shows the binary image, the midpoint obtained by the center of gravity method, the midpoint obtained by the inscribed parallelogram method.

What the defect is that it can not make inscribed parallelogram and is unable to find the center when the block is over the center line of the ellipse. The improvement is given below.

When the eyelids block over the center line of the ellipse, the edge pixels of the pupil is not suitable for computing the center of the inscribed parallelogram. The center we find is wrong, as shown in Fig. 8. So it needs to rotate the line according to the angle of the boundary line formed by the eyelids and the pupil into a horizontal line direction. Then find the center by the method described above, and finally rotate the center reversely to the correct location with the angle.

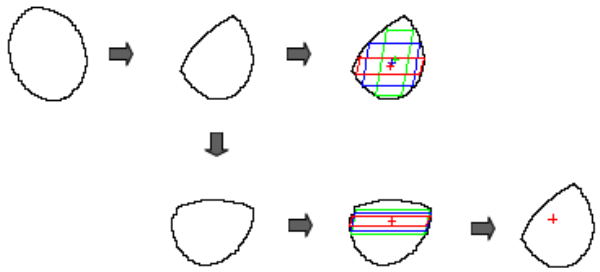

Figure 8. On the upper row, the eyelids block over the center line of the ellipse, and the center of the parallelograms inscribed on the ellipse is wrong. On the lower row, the ellipse is rotated first, and then the center obtained of the parallelogram inscribed on the ellipse is correct.

We take the following steps to compute the angle, as shown in Fig. 9. First make the circumscribed quadrilateral of the segmented deformed ellipse, and find the four tangent points. And then take five edge points to fit an ellipse, and estimate the approximate center position. Last determine the two cut points as the intersection point of the eyelid and the pupil under the level or vertical distance between tangent point and the center, and calculate the rotation angle.

Figure 9. The figure shows, from left to right, the binary deformed ellipse, the circumscribed quadrilateral (blue quadrilateral) of the segmented deformed ellipse together with the connection of the intersection point of the eyelid and the pupil (red wire), the deformed ellipse after rotation.

The cut point is the approximation of the intersection of the eyelid and pupil, making the margins of error between the angle formed by the connection of the two cut points and the angle of the real boundary. Consider that this measure is only to rotation graph to facilitate the calculation of the ellipse center by parallelogram, and the center is of the many overlapping point meantime, it do not have much impact on the selection of the center when the rotation angle of deviation is not the case, which meet the general situation.

D. Calculation of Pupil Diameter

First, the ellipse equation is formulated from the points located on the obtained outline of the ellipse. An ellipse equation can be shown in the form of (1) [7].

$$Ax^2 + Bxy + Cy^2 + Dx + Ey + F = 0 \quad (1)$$

Parameters A-F from (1) are calculated with the method of Gauss Elimination from five points. The five points are chosen from the points on the outline of the ellipse for calculating the pupil center and pupil diameter in accordance with the following principles. Get the lowest point as one candidate point first of all. Then climb up to a quarter of the outline from the bottom and get the left and right points as another two candidate points. Again climb up to half of the outline and get the left and right points as another two candidate points. Thus we have five points. The coordinates of the ellipse center are solved using (2) and (3).

$$x_0 = \frac{BE - 2CD}{4AC - B^2} \quad (2)$$

$$y_0 = \frac{BD - 2AE}{4AC - B^2} \quad (3)$$

If these coordinates of the ellipse center is the same as the coordinates obtained by parallelograms, the five points are chosen. Otherwise, select another five points. Keep holding the lowest point, and move the other four points downhill, until meet the demands. After getting the five right points, the major axis, the minor axis and the angle are calculated using (4), (5), and (6), respectively.

$$a = \sqrt{\frac{2(Ax_0^2 + Bx_0y_0 + Cy_0^2 - F)}{(A+C) - \sqrt{B^2 + (A-C)^2}}} \quad (4)$$

$$b = \sqrt{\frac{2(Ax_0^2 + Bx_0y_0 + Cy_0^2 - F)}{(A+C) + \sqrt{B^2 + (A-C)^2}}} \quad (5)$$

$$fangle = 0.5 \times a\tan\left(\frac{B}{A-C}\right) \quad (6)$$

In the end, the occluded ellipse is able to be renewed with the paramaters of the center, the major axis, the minor axis and the angle, as shown in Fig. 10.

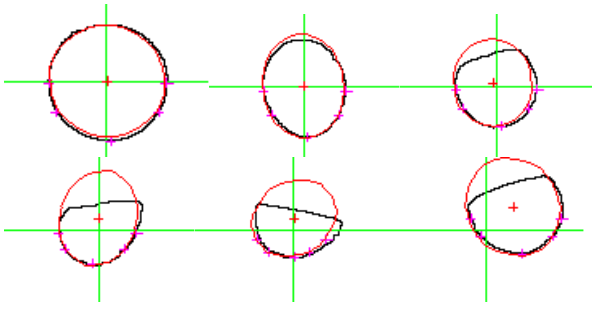

Figure 10. The pupil fitted by five points eliminating the impact of occlusion.

The selection of the five points has a significant impact on the fitting of the ellipse. They are chosen to achieve the target we want. When the occlusion does not exceed the center line of the un-rotated ellipse, the five points adapted according to the method described above are nice for processing. When the occlusion exceeds the center line of the un-rotated ellipse, the center of the rotated ellipse can not be found, the five points are wrong. Therefore, another five points should be reconsidered. Get the lowest point again, then climb up to one-eight of the outline from the bottom and get the left and right points as another two candidate points. Again climb up to a quarter of the outline and get the left and right points as another two candidate points. If the five points are not meet the above rules, keep holding the lowest point, and move the other four points downhill, until the conditions are met. When the occlusion takes up most of the areas, consider giving up the fitting or choosing the five points near the bottom at random to fit the ellipse as the final result at the expense of the accuracy to achieve stability. Fig. 11 shows the results of the pupil center and radius detection.

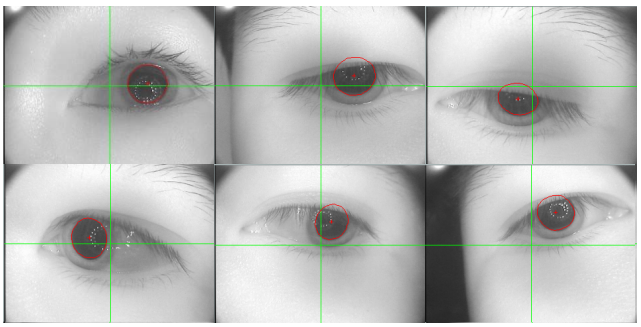

Figure 11. Results of pupil center and radius detection. The upper row and the lower row describe two tests while the pupil is positive and oblique.

IV. Conclusion

A robust and accurate algorithm for pupil center and radius estimation for the screening of diabetic retinopathy is described in this paper. Test results on pupil area measurement show that the algorithm we proposed has a good performance in terms of a more accurate measurement of the pupil size under interference, such as eye corners and eyelid occlusion. The algorithm can effectively deal with the case that the occlusion area is about half of the whole pupil area, and satisfies the real time requirement.

Acknowledgment

This work is supported by the Key Project for National Natural Science Foundation of China (No. 60827002).

References

[1] Anja B. Hansen, Birgit Sander, Michael Larsen, "Screening for diabetic retinopathy using a digital non-mydriatic camera compared with standard 35-mm stereo colour transparencies," Acta Ophthalmologica Scandinabica, 2004,2:656-665.

[2] GORIN, Michael B., "Method and apparatus for screening for retinopathy," Patent filed internatinally, 2006, information available at:

http://www.wipo.int/pctdb/en/wo.jsp?wo=2006041625&IA=WO2006041625&DISPLAY=STATUS.

[3] Khalid Al Sabti, Seemant Raizad, Vivek B. Wani, Mubarak Al Ajmi, Iskender Gayed, T.N.Sugathan, "Efficacy and reliability of fundus digital camera as a screening tool for diabetic retinopathy," in Kuwait, Journal of Diabetes and Its Complications, 2003;17: 229–233.

[4] J. Kim, K. Park and G. Khang, "A method for size estimation of amorphous pupil in 3-dimensional geometry", Proceedings of the 26th Annual International Conference of the IEEE EMBS, vol. 1, Sept. 2004, pp.1451-1454.

[5] D. Hansen and A. Pece, "Eye tracking in the wild," Computer Vision and Image Understanding, vol.98, no.1,pp.155–181,2005.

[6] Y. Sakashita, H. Fujiyoshi, "Accurate and fast ellipse detection for pupil extraction," East Sea of society related to electricity in 2005 fiscal year branch union rally, O-250(2005).

[7] T. Tsuji, "Iris detection using LMedS for eye tracking system," MIRU2004,I-684(2004.7).